PLOS ONE

RESEARCH ARTICLE

Development of a novel *Francisella tularensis* Live Vaccine Strain expressing ovalbumin provides insight into antigen-specific CD8$^+$ T cell responses

David E. Place[¤a☯], David R. Williamson[☯], Yevgeniy Yuzefpolskiy[¤b], Bhuvana Katkere, Surojit Sarkar[¤b], Vandana Kalia[¤b], Girish S. Kirimanjeswara*

Department of Veterinary and Biomedical Sciences, Pennsylvania State University, University Park, Pennsylvania, United States of America

☯ These authors contributed equally to this work.
¤a Current address: Department of Immunology, St Jude Children's Research Hospital, Memphis, Tennessee, United States of America
¤b Current address: Ben Towne Center for Childhood Cancer Research, Seattle Children's Hospital, Seattle, Washington, United States of America
* gsk125@psu.edu

OPEN ACCESS

Citation: Place DE, Williamson DR, Yuzefpolskiy Y, Katkere B, Sarkar S, Kalia V, et al. (2017) Development of a novel *Francisella tularensis* Live Vaccine Strain expressing ovalbumin provides insight into antigen-specific CD8$^+$ T cell responses. PLoS ONE 12(12): e0190384. https://doi.org/10.1371/journal.pone.0190384

Editor: Ashlesh K Murthy, Midwestern University, UNITED STATES

Received: October 7, 2017

Accepted: December 13, 2017

Published: December 28, 2017

Data Availability Statement: All relevant data are within the paper and its Supporting Information files.

Funding: This work was supported by the National Institutes of health, AI077917 and AI074551 (https://www.nih.gov) and the US Department of Agriculture AES, AES 4605 (https://www.usda.gov). The funders had no role in study design, data collection and analysis, decision to publish, or preparation of the manuscript.

Abstract

Progress towards a safe and effective vaccine for the prevention of tularemia has been hindered by a lack of knowledge regarding the correlates of protective adaptive immunity and a lack of tools to generate this knowledge. CD8$^+$ T cells are essential for protective immunity against virulent strains of *Francisella tularensis*, but to-date, it has not been possible to study these cells in an antigen-specific manner. Here, we report the development of a tool for expression of the model antigen ovalbumin (OVA) in *F. tularensis*, which allows for the study of CD8$^+$ T cell responses to the bacterium. We demonstrate that in response to intranasal infection with the *F. tularensis* Live Vaccine Strain, adoptively transferred OVA-specific CD8$^+$ T cells expand after the first week and produce IFN-γ but not IL-17. Effector and central memory subsets develop with disparate kinetics in the lungs, draining lymph node and spleen. Notably, OVA-specific cells are poorly retained in the lungs after clearance of infection. We also show that intranasal vaccination leads to more antigen-specific CD8$^+$ T cells in the lung-draining lymph node compared to scarification vaccination, but that an intranasal booster overcomes this difference. Together, our data show that this novel tool can be used to study multiple aspects of the CD8$^+$ T cell response to *F. tularensis*. Use of this tool will enhance our understanding of immunity to this deadly pathogen.

Introduction

The Gram-negative bacterium, *Francisella tularensis*, is the etiological agent of the disease tularemia in humans. Inhalation of approximately 10–50 CFU [1] of *F. tularensis* subsp. *tularensis* can lead to severe and rapidly-progressing disease, which is associated with high mortality

Competing interests: The authors have declared that no competing interests exist.

without early intervention [2]. Additionally, the bacterium is easily aerosolized [3], and can be genetically manipulated to render it antibiotic resistant. The combination of these factors makes *F. tularensis* an ideal candidate biological weapon. Indeed, it was developed for this purpose by several countries in the 20th century [2,4–6], and remains a tier 1 select agent due to the potential for use as an agent of bio-terrorism.

There is currently no approved vaccine for the prevention of tularemia. An empirically attenuated Live Vaccine Strain (LVS), derived from a *F. tularensis* subsp. *holarctica* isolate, was developed over 50 years ago [7]. The exact basis of attenuation, however, is still not well defined; this and the potential for either loss of protectiveness [8,9] or reversion to virulence [10,11] are barriers for the approval of LVS for vaccination in humans. Additionally, the effectiveness of LVS in generating long term protection from respiratory challenge with virulent strains is poor in many models [12–14]. To facilitate the development and approval of a vaccine that is safe and effective, it is crucial that the correlates of protective adaptive immunity to *F. tularensis* be clearly defined.

Antibody-mediated immunity appears to be a poor correlate of immunity to highly virulent *F. tularensis* strains; antibody titers do not correlate with protection in humans[15], and the transfer of immune serum fails to protect recipient mice against the challenge with virulent strain of *F. tularensis* [16–18]. In contrast, both $CD4^+$ and $CD8^+$ T cells are known to be required for protection, as depletion of either subset abolishes protective immunity [12,19,20]. To truly hone in on correlates of protective T cell responses, it is necessary to be able to differentiate cells specifically responding to the pathogen of interest from cells of other specificities [21]. These non-specific cells may be far more abundant than pathogen-specific cells, thus representing a significant level of 'background noise' that may mask important insights into the true response to the pathogen. Antigen-specific cells can be studied by staining with MHC-peptide tetramers [22], or by tracking adoptively transferred transgenic T cells that are specific for a pathogen epitope. Thus far, there has been no success in using MHC-peptide tetramers to track T cells specific to natural *F. tularensis* antigens and no TCR-transgenic mice that recognize *Francisella*-specific epitopes have been generated. An alternative approach involves engineering strains of *F. tularensis* that express model antigens, which can be studied using existing tools.

In this regard, Roberts et al. have developed a construct in which they express the *F. tularensis* protein IglC tagged with the gp61-80 epitope of LCMV, allowing for tracking of antigen-specific $CD4^+$ T cell responses using MHC-II tetramers [20]. This tool has allowed investigators to characterize antigen-specific $CD4^+$ T cells in various contexts and begin identifying the correlates of CD4-mediated protection from tularemia. For instance, a protective vaccine leads to more antigen-specific $CD4^+$ T_{EM} in the mediastinal lymph node (MLN) and spleen, as compared to a non-protective vaccine [20]. Additionally, the tool has been used to study how these cells respond to a prime-boost strategy [13] and has revealed the dramatic influence high avidity $CD4^+$ T cell epitopes have on protection [13,20]. While this tool will undoubtedly yield many more insights into the role of $CD4^+$ T cells in immunity to *F. tularensis*, no such tool currently exists to characterize $CD8^+$ T cells, which are also required for protection against this predominantly intracellular pathogen [12,19,20].

To address this shortcoming, we have developed a tool for expression of chicken ovalbumin (OVA) protein in *F. tularensis*. This tool makes it possible to study the response of OT-I (TCR-transgenic) $CD8^+$ T cells [23], which can be adoptively transferred into congenic C57BL/6 mice. Here we report the development of this tool and a proof-of-concept study using OVA-expressing *F. tularensis* LVS (termed LVS-OVA). In response to LVS-OVA, OT-I $CD8^+$ T cells proliferate, differentiate into effector and central memory subsets, and produce interferon gamma (IFN-γ). We also compare how these cells respond following intranasal or scarification

vaccination with LVS-OVA, followed by an intranasal booster. This novel tool will enable further detailed studies into the CD8+ T cell response to *F. tularensis*.

Materials and methods

Mouse strains

C57BL/6J (Thy1.2+), C57BL/6J Thy1.1+ congenic mice (B6.PL-Thy1a/CyJ), and OT-I (C57BL/6-Tg(TcraTcrb)1100Mjb/J), mice were purchased from The Jackson Laboratories (Bar Harbor, ME). Unless otherwise indicated, experiments were performed using 6–8 weeks old heterozygous wild-type Thy1.1+/Thy1.2+ recipient mice with sex-matched OT-I (Thy1.1-/Thy1.2+) donor splenocytes. Experimental groups consisted of both male and female mice. All mice were maintained in specific pathogen-free conditions at the Pennsylvania State University animal care facilities and had unlimited access to food and water.

Bacterial strains and cell culture

Cloning was performed using *Escherichia coli* DH5α grown at 37˚C in LB broth or LB agar containing tetracycline or kanamycin (10μg/mL or 50μg/mL, respectively). *Francisella tularensis* Live Vaccine Strain (LVS), obtained from Albany Medical College, was grown shaking in BHI broth at 37˚C or on modified Mueller-Hinton II agar supplemented with hemoglobin (Thermo Scientific) and IsoVitalex (BD Biosciences) at 37˚C in 5% CO_2 with tetracycline or kanamycin (2μg/mL or 10μg/mL, respectively). For allelic exchange, Km^R LVS primary recombinants were streaked out on plates containing 5% sucrose and resulting colonies were screened for secondary recombination by plating single colonies on antibiotic-free, ampicillin, or kanamycin plates as previously described [24]. Mid-log phase liquid cultures of LVS were frozen at -80˚C directly in BHI and enumerated regularly to calculate doses for mouse inoculation.

For immunoblots, liquid cultures (OD_{600} ~0.10) were pelleted and resuspended in bacterial lysis buffer followed by sonication. Lysate was mixed with 5X Laemelli buffer (BioRad) before running on 12% pre-cast Criterion TGX gels (BioRad). Protein was transferred to PVDF membrane using the Trans-Blot Turbo mixed molecular weight program. Membranes were then blocked in 5% BSA/TBS-T for 1h at room temperature, probed with anti-6xHis-Biotin (1:5000, Rockland #600-406-382) in 5%BSA/TBS-T for 1h at room temperature, washed, and probed with a secondary streptavidin-HRP (1:50000, Jackson ImmunoResearch) for 1h at room temperature. Blots were developed using Millipore Immobilon Chemiluminescent Substrate and images were collected on a BioRad ChemiDoc XRS+.

Plasmids

Plasmid pKK214 containing GFP was obtained from Dr. Karl Klose and the GFP gene was removed by restriction digestion and replaced with a cloning site containing XbaI restriction sites. LVS genomic DNA was used to amplify the promoter for the bacterioferritin gene (*bfrp)* by PCR and to introduce flanking XbaI and BamHI restriction sites. The complete *vgrG* gene was amplified with primers introducing a BamHI site and replacing the stop codon with an XhoI site. To generate the codon-optimized ovalbumin epitope tag (containing OVA amino acids 239–345, a 6xHis tag, stop codon, and flanking XhoI and XbaI sites), the LVS codon frequency table from the Codon Usage DB (http://www.kazusa.or.jp/codon/cgi-bin/showcodon.cgi?species=376619) was imported into OPTIMIZER (genomes.urv.es/OPTIMIZER) using the standard setting of "one amino acid–one codon" [25]. The codon-optimized sequence was submitted for synthesis to Integrated DNA Technologies as a gBlock Gene Fragment, cloned into pCR4 cloning vector (Invitrogen) and confirmed by sequencing by the Penn State Genomics

Core Facility. The bacterioferritin promoter, vgrG, and $OVA_{239-345}$-6xHis fragments were ligated with T4 DNA ligase (NEB) and cloned into XbaI-digested pKK214 to generate pKK214-vgrG-OVA or pKK214-OVAgB. Electroporation was used to introduce plasmids to *E. coli* and LVS. A summary of primers, plasmids, and strains used can be found in Table 1.

Adoptive transfer

For adoptive transfer of OT-I splenocytes ($Thy1.1^-/Thy1.2^+$), sex-matched spleens were aseptically collected in RPMI 1640 containing 10% FBS, 2mM L-glutamine, 1mM sodium pyruvate, 1x non-essential amino acids, 10mM HEPES, 55μM beta-mercaptoethanol and penicillin/streptomycin. Spleens were passed through a 70μm mesh filter by crushing with a 3mL syringe plunger and pelleted. Red blood cells were lysed with sterile 0.84% ammonium chloride/EDTA/Sodium bicarbonate and washed with complete media. For experiments with CFSE-labelled splenocytes, cells were washed with plain RPMI 1640 before resuspension at a concentration of 10^7 cells/mL in RPMI 1640 containing 5μM CFSE. Staining was quenched by addition of 10% FBS and cells were washed twice with complete RPMI. $5x10^6$ OT-I splenocytes were transferred to $Thy1.1^+/Thy1.2^+$ recipients by intraperitoneal injection 24h before bacterial inoculation.

Mouse infection

Mouse inoculation was performed by thawing enumerated frozen bacterial stocks and serially diluting in PBS to the desired dose, which was 1000 CFU for standard intranasal experiments, 10,000 CFU for intranasal boosters, and 100,000 CFU for skin scarification. For intranasal inoculation, mice were lightly anesthetized using isoflurane and a 50μL droplet was administered to the external nares and inhaled. For skin scarification, mice were anesthetized using isoflurane, the fur of the upper back was shaved, and the skin cleaned by wiping with 70% ethanol. After drying, a 10μL droplet was administered to the bare skin, and a sterile bifurcated needle (Precision Medical Products) used to prick the skin 15 times. Mice were euthanized by CO_2 inhalation and dissected aseptically in a biosafety cabinet. For experiments including bacterial burden determination, serial dilutions of single cell suspensions were prepared as described below, and plated on modified Mueller-Hinton agar plates. Mice were closely monitored and body weight was measured daily with an end point set at a loss of 20% or more initial body weight or any other signs of severe distress.

Flow cytometry and intracellular cytokine staining

Mice were euthanized and cold PBS was used to perfuse tissues by cardiac injection. The caudal mediastinal lymph node (MLN) and spleen were collected in HBSS with 1.3mM EDTA and crushed with a 3mL syringe plunger through a 70μm nylon filter. Lungs were collected, minced, suspended in HBSS with 1.3mM EDTA, and shaken 30 min. at 37˚C. Following this, lungs were pelleted, resuspended in complete RPMI containing 200U/mL collagenase type I (Worthington Biochemical Corporation) and shaken at 37˚C for 1h before passing through a 70μm nylon filter. Spleen and lung cells were treated with RBC lysis solution and washed with PBS/2%FBS. For surface staining, cells were incubated with relevant antibodies for 30 min on ice, washed, and fixed in PBS/1% PFA prior to running on a BD LSR Fortessa at Penn State Microscopy and Cytometry Facility. Intracellular cytokines were analyzed by stimulating ~2-$10x10^6$ cells in 96-well plates at 37˚C and 5% CO_2 in the presence of 1xBrefeldin A (BioLegend) alone (unstimulated), or with 8nM phorbol 12-myristate 13-acetate (PMA) (Sigma) / 500ng/mL Calcium Ionophore A23187 (Sigma #C7522) for 4h in complete RPMI. Cells were stained for extracellular markers as above, fixed, then permeabilized with 0.1% saponin in PBS/2%FBS. Antibodies for intracellular cytokines were incubated 30min in permeabilization

Table 1. Summary of primers, plasmids and bacterial strains used in this study.

Strain or plasmid	Description	Reference or source
***E. coli* strains**		
DH5α	F– Φ80*lac*ZΔM15 Δ(*lac*ZYA-*arg*F) U169 *rec*A1 *end*A1 *hsd*R17 (rK–, mK+) *pho*A *sup*E44 λ– *thi*-1 *gyr*A96 *rel*A1	Life Technologies
***F. tularensis* strains**		
LVS	*F. tularensis* subsp. *holarctica* live vaccine strain	Albany Medical College
LVS-OVA	LVS carrying pKK214-vgrG-OVA	This study.
Plasmids		
pCR4-TOPO	Ap^R, Km^R, cloning vector	Invitrogen
pKK214	Tc^R, E. coli-F. tularensis shuttle vector	[26,27] and Karl Klose
pKK214-vgrG-OVA	Tc^R, pKK214 containing *bfrp-vgrG-OVA-6xHis*	This study.
Primers and DNA		
Bfr_fwd (XbaI)	CAATACTGCATCTAGAGATCCATACCCATGATGGTTAC	For ligation with pKK214
Bfr_rev (BamHI)	GCCGCGGGATCCTATTGTTACCTCCATTATTTAAAACTCTAATCA	For ligation with vgrG
vgrG_fwd (BamHI)	TATGGATCCATGTCAAAAGCAGACCATAT	For ligation with *bfrp*
vgrG_rev (XhoI)	GATCTCGAGTCCAACCATTGTTGCTGTAGA	For ligation with OVAgB
OVA gBlock	AGATATTCTAGACTCGAGGGATCCATGTCAATGTTAGTTTTATTACCAGATGAAGTTTCAGGTTT AGAACAATTAGAATCAATTATTAATTTTGAAAAATTAACTGAATGGACTTCATCAAATGTTATGG AAGAAAGAAAAATTAAAGTTTATTTACCAAGAATGAAAATGGAAGAAAAATATAATTTAACTTCA GTTTTAATGGCTATGGGTATTACTGATGTTTTTTCATCATCAGCTAATTTATCAGGTATTTCATC AGCTGAATCATTAAAAATTTCACAAGCTGTTCATGCTGCTCATGCTGAAATTAATGAAGCTGGTA GAGAAGTTGTTGGTTCAGCTCATCATCATCATCACCATTAACTCGAGTCTAGAGAGCTCTATAGA	Integrated DNA Technologies
OVAgB_fwd (XhoI)	TATCTCGAGATGTCAATGTTAGTTTTATTACC	For ligation with *vgrG*
OVAgB_rev (XbaI)	ATATCTAGAGAGCTCTTAATGGTGATGATGATG	For ligation with pKK214

https://doi.org/10.1371/journal.pone.0190384.t001

buffer, washed 3x with permeabilization buffer then 3x with PBS/2%FBS, and analyzed immediately. Analysis was performed using FlowJo v10.0.8 software (company). In all cases, gates were set for single cells (FSC-A/FSC-H and SSC-A/SSC-H), followed by a lymphocyte gate (FSC-SSC). $CD8^+$ OT-I cells were differentiated from endogenous CD8+ cells by gating based on Thy1.1 and Thy1.2. The antibodies used were as follows, all purchased from BioLegend: CD8a-PerCP-Cy5.5 (53–6.7), Thy1.1-AF488 or -PE (OX-7), Thy1.2-BV510 (53–2.1), CD44-APC-Cy7 (IM7), CD62L-PE-Cy7 (MEL-14), IFNγ-PE (XMG1.2), IL-17A-PE-Cy7 (TC11-18H10), CD103-APC(2E7), CD69-PE(H1.2F3).

Statistical analysis

Statistical tests were performed as indicated in figure legends using GraphPad Prism 5.0.

Ethics statement

All animal experiments were carried out by following recommendations and approval from the Pennsylvania State University Animal Care and Use Committee (protocols 45613, 45794 & 46070) with great care taken to minimize suffering of animals.

Results

Generation of *F. tularensis* LVS expressing OVA

We sought to constitutively express a fragment of the chicken ovalbumin protein, $OVA_{239-345}$, in *F. tularensis* LVS in order to characterize the development and maintenance of antigen-

specific CD8$^+$ T cells in mice. A codon-optimized OVA$_{239\text{-}345}$ tethered to a 6X- histidine tag at the C terminal end was ligated to the 3' end of *vgrG* downstream of the highly active bacterioferritin promoter [28], generating pKK214-vgrG-OVA (Fig 1A). This was introduced into *F. tularensis* LVS, and expression determined by immunoblot of bacterial lysates using anti-6X histidine antibody. As shown in Fig 1B, a high level of expression of vgrG-OVA$_{239\text{-}345}$ was observed. Despite previous work showing that pKK214 plasmids are stably maintained without selection [29], we assessed the stability of pKK214-vgrG-OVA without selection i*n vivo*. Similar numbers of wild-type LVS, LVS-harboring empty vector pKK214, and LVS-OVA were recovered from the lungs of separate sets of mice on days 3 and 7 following infection with 1,000 cfu of each strain (Fig 1C). The presence or absence of tetracycline in culture plates did not affect the number of colonies of LVS-pKK214 or LVS-OVA recovered from infected mice (Fig 1C). These data show that our pKK214-vgrG-OVA expression construct allows LVS to express high levels of OVA and that the plasmid is robustly maintained without antibiotic selection *in vivo*.

Antigen-specific proliferation of CD8$^+$ OT-I cells in response to LVS-OVA

To test the ability of LVS-OVA to activate antigen-specific OT-I (CD8$^+$) cells, we utilized an adoptive transfer model utilizing wild-type Thy1.1$^+$ /Thy1.2$^+$ congenic recipient mice. One day prior to infection with LVS-OVA, 5x10^6 OT-I splenocytes (Thy1.1$^-$/Thy1.2$^+$) were transferred into wild-type congenic mice by intraperitoneal injection. Prior to injection, OT-I splenocytes were stained with CFSE, a bright and stable dye that is diluted with each round of cell division [30,31]. On days 5, 7, and 9 post-inoculation with LVS-pKK214 (vector control) or LVS-OVA, the lungs, lung-draining mediastinal lymph nodes (MLN), and spleens were collected and analyzed by flow cytometry. LVS-OVA led to robust proliferation of OVA-specific OT-I cells, while LVS-pKK214 stimulated comparatively little expansion (Fig 2A–2C). By day 7 post-inoculation, many CFSE$^+$ OT-I cells appeared to have undergone at least 5 rounds of cell division (Fig 2B). On day 9, OT-I cells represented the majority of the CD8$^+$ T cells present in the lung (~60%) and a large proportion of the spleen (~25%), but were not as abundant in the MLN, suggesting that upon activation OT-I cells largely migrate out of the MLN (Fig 2C). Together, these data show that LVS-OVA specifically activates OT-I T cells and can be used to study CD8$^+$ T cell responses to *Francisella*.

Kinetics of the CD8$^+$ T cell response to intranasal LVS infection

To-date, it has not been possible to track the antigen-specific CD8$^+$ T cell response in the context of *F. tularensis* infection/vaccination, due to a lack of tools to differentiate specific cells from the broader CD8$^+$ population. After adoptively transferring OT-I cells and infecting intranasally with LVS-OVA, we measured the number of OVA-specific CD8$^+$ T cells in the lungs, MLN and spleen before infection, during infection and following bacterial clearance (Fig 3). Peak bacterial burdens were observed between day 3–7 post-infection, with far lower burdens evident on day 14, and clearance by day 21 (Fig 3A). There were relatively very few OT-I cells in the lungs and MLNs (~10^2 cell per organ) of recipient mice 24hr after the transfer and before infection. However, a much larger number of OT-I cells (~10^4 per organ) were detected in the spleens of mice at that time. We observed a pattern similar to other pathogens where the T cell response peaks, then rapidly contracts after the infection is cleared. The scale and speed of contraction was greatest in the lungs; with a reduction in the number of OT-I cells from day 7 to all later time points (Fig 3B). In the MLN and spleen, contraction was more gradual, with retention of a greater proportion of OT-I cells through day 71 (Fig 3C and 3D).

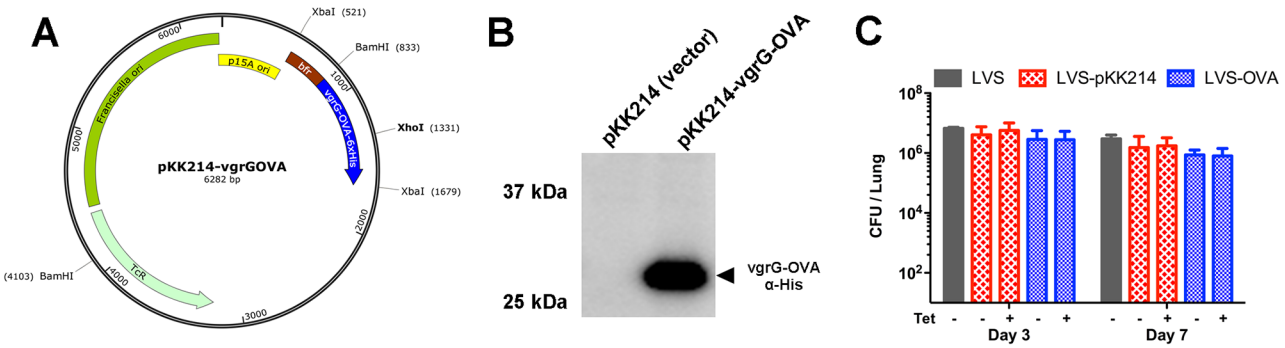

Fig 1. Generation and stability of LVS-OVA. A) Map of the pKK214-vgrG-OVA plasmid. B) Immunoblot demonstrating expression of the VgrG-OVA construct by cells harboring plasmid (pKK214-vgrG-OVA). C) Stability of the pKK214-vgrG-OVA plasmid during an *in vivo* infection. C57BL/6J mice (n = 3 per group) were infected with 1000 CFU of wild-type *F. tularensis* LVS, LVS harboring empty vector (LVS-pKK214), or LVS harboring pKK214-vgrG-OVA (LVS-OVA). Serial dilutions of lung homogenates were plated with or without tetracycline as indicated.

https://doi.org/10.1371/journal.pone.0190384.g001

These data suggest that antigen-specific T cells are retained poorly in the lungs compared to secondary lymphoid organs, even following intranasal LVO-OVA vaccination.

LVS-OVA can be used to study antigen-specific CD8+ T cell cytokine responses in *F. tularensis* infection

One of the primary effector functions of CD8+ T cells is the production of inflammatory cytokines. Activated CD8+ T cells are capable of producing a range of cytokines depending on inflammatory cues and transcriptional programing [32,33]. Among these, IFN-γ is known to play an important role in activating phagocytic cells to kill intracellular pathogens including *F. tularensis*, and has shown to be produced by CD8+ T cells in response to the bacterium [34–36]. In contrast, IL-17A is only produced by CD8+ T cells in rare cases; its production by OT-I cells would not be expected in response to *F. tularensis*, thus we expected it may be useful as a negative control. To test the utility of LVS-OVA in studying the cytokines produced by CD8+ T cells responding to *F. tularensis* infection, we performed intracellular cytokine staining on cells isolated from LVS-OVA-infected animals and stimulated with PMA/calcium ionophore.

As expected, we observed that some CD8+ OT-I cells produced IFN-γ during and after infection with LVS-OVA (Fig 4A). For each organ, the peak in IFN-γ producing cells coincided with peak T_{EM} responses (see below), and occurs around the time the immune response is beginning to contain bacterial burden. We did not observe any significant production of IL-17A by stimulated OT-I cells at any time-point during infection (Fig 4B). These results show that LVS-OVA can be used to study antigen-specific CD8+ T cell cytokine responses in *F. tularensis* infection.

Antigen-specific CD8+ memory T cell development in response to LVS-OVA

Upon activation, naïve CD8+ T cells differentiate into effector and memory subsets. Effector/memory (T_{EM}) CD8+ T cells are characterized by the decreased expression of markers associated with lymphoid tissue homing (eg: CD62L) and increased expression of markers associated with homing to the source of inflammation (eg: CD44) [37]. These cells have a high propensity for effector functions, including killing infected cells and producing cytokines. Central memory (T_{CM}) cells are less geared towards effector functions; rather they retain extensive

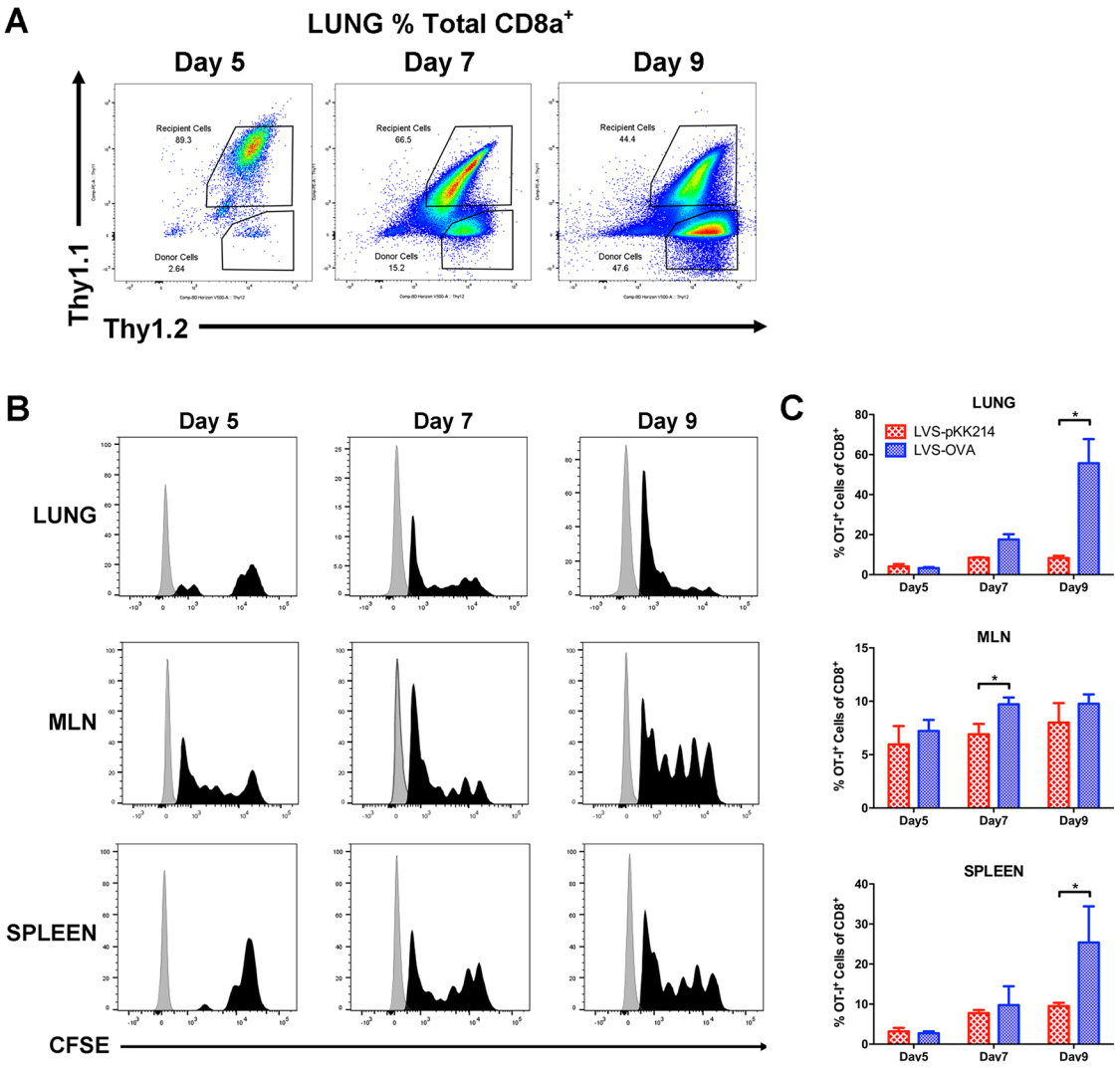

Fig 2. Antigen-specific proliferation of CD8+ OT-I cells in response to LVS-OVA. Thy1.1-/Thy1.2+ OT-I cells were transferred in to Thy1.1+/Thy1.2+ recipient mice, 24 hours prior to infection with 1000 CFU of LVS-OVA or LVS-pKK214 (LVS with empty vector). A) representative scatterplots of CD8+ cells from the lungs of animals infected with LVS-OVA. B) CFSE dilution of CD8+ OT-I cells isolated from animals infected with LVS-OVA. C) The frequency of CD8+ OT-I cells in animals infected with LVS-OVA or LVS-pKK214. n = 3 per group, means +/- SD are plotted; * p<0.05 according to two-tailed, unpaired T test.

https://doi.org/10.1371/journal.pone.0190384.g002

proliferative capacity, and primarily circulate through the secondary lymphoid organs due to high expression of CD62L and other lymphoid tissue homing markers [37]. The primary role of T_{CM} is generally considered to be their ability to rapidly expand into a new population of effector cells upon re-exposure to antigen [38,39]. Using our model, we monitored the OVA-specific T_{EM} and T_{CM} subsets that arose in the lungs, MLN and spleen in response to intranasal LVS-OVA infection.

In the lungs, the highest number of effector memory OT-I cells were observed on day 7 (Fig 5B), which coincides with the peak bacterial burden in this assay (Fig 3A). T_{EM} remained at high levels in the lung to the time of clearance then dropped sharply in number, with only a small number detected on d28 post-infection. In the MLN, T_{EM} numbers followed a similar

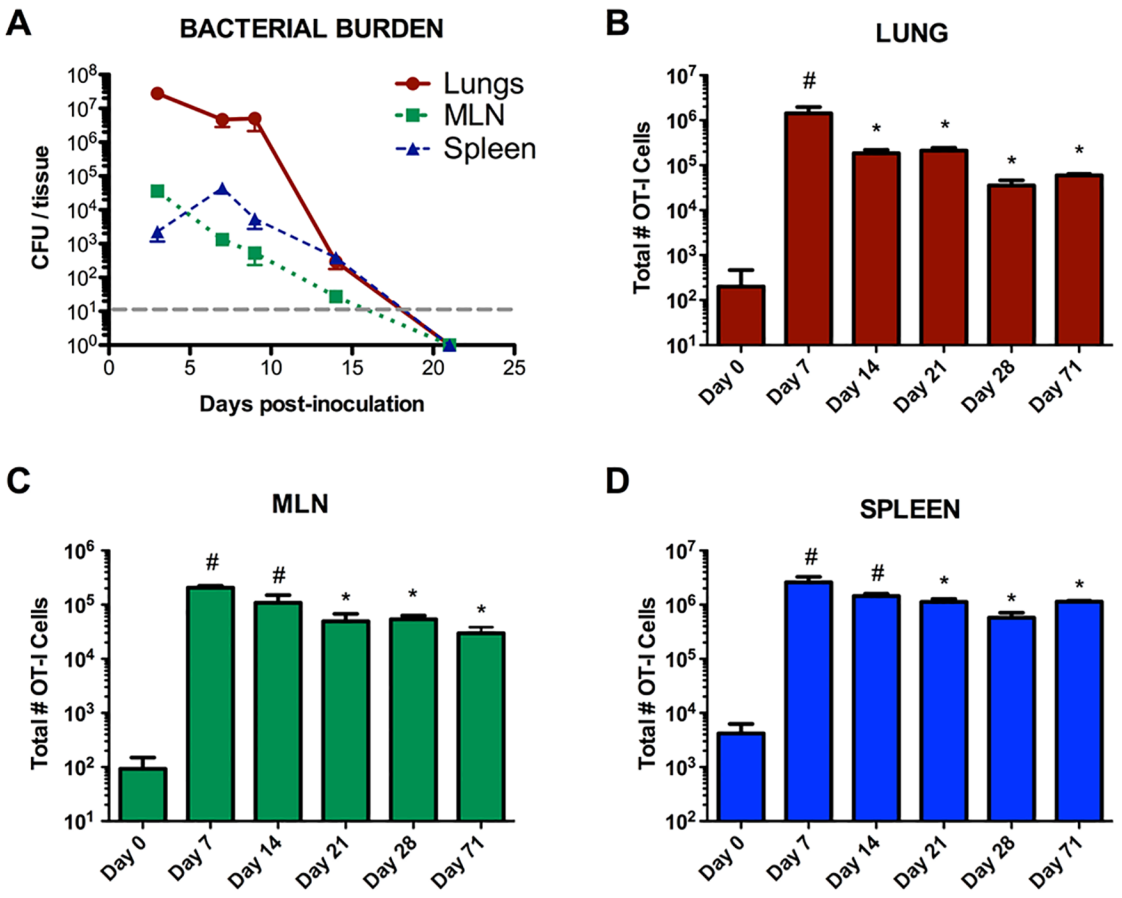

Fig 3. Kinetics of the CD8+ T cell response to intranasal LVS infection. OT-I cells were adoptively transferred into recipient mice 24 hours prior to infection with 1000 CFU of LVS-OVA. A) Bacterial burden of infected animals over time. B-D) number of CD8+ OT-I cells in infected animals over time. Day 0 data are for uninfected mice 24h after adoptive transfer. n = 3 per group, means +/- SEM are plotted. Statistical significance ($p<0.05$) for one-way ANOVA with Tukey's post test, for the indicated column compared to: # day 0, * day 7.

https://doi.org/10.1371/journal.pone.0190384.g003

general pattern as in the lung, with the most cells present on day 7; however, a transient increase was observed on day 28, possibly reflecting egress of these cells out of the lung (Fig 5B). In contrast to the lungs and MLN, T_{EM} peaked in number on day 14 in the spleen (Fig 5B). This may be due to the fact that bacteria reach the spleen and replicate later in the course of pneumonic tularemia compared to the lungs (Fig 3A and [40,41]). Consistent with the data for total OT-I cells (Fig 3), OT-I T_{EM} are retained well in the spleen and poorly in the lungs after bacterial clearance.

As expected, the number of T_{CM} in the lung was much lower than the number of T_{EM} during infection, and remained similar from day 7 to day 28 (Fig 5C). The number of T_{CM} in the MLN peaked on day 14, then exhibited a trend towards gradual decrease over time. In the spleen, T_{CM} increased in number between day 7 and 21, and decreased on day 28 (Fig 5C). These data show that our LVS-OVA/OT-I model can be used to monitor antigen-specific CD8+ T cell memory subsets, and that these subsets show disparate expansion, contraction and retention properties in various tissues following intranasal LVS infection.

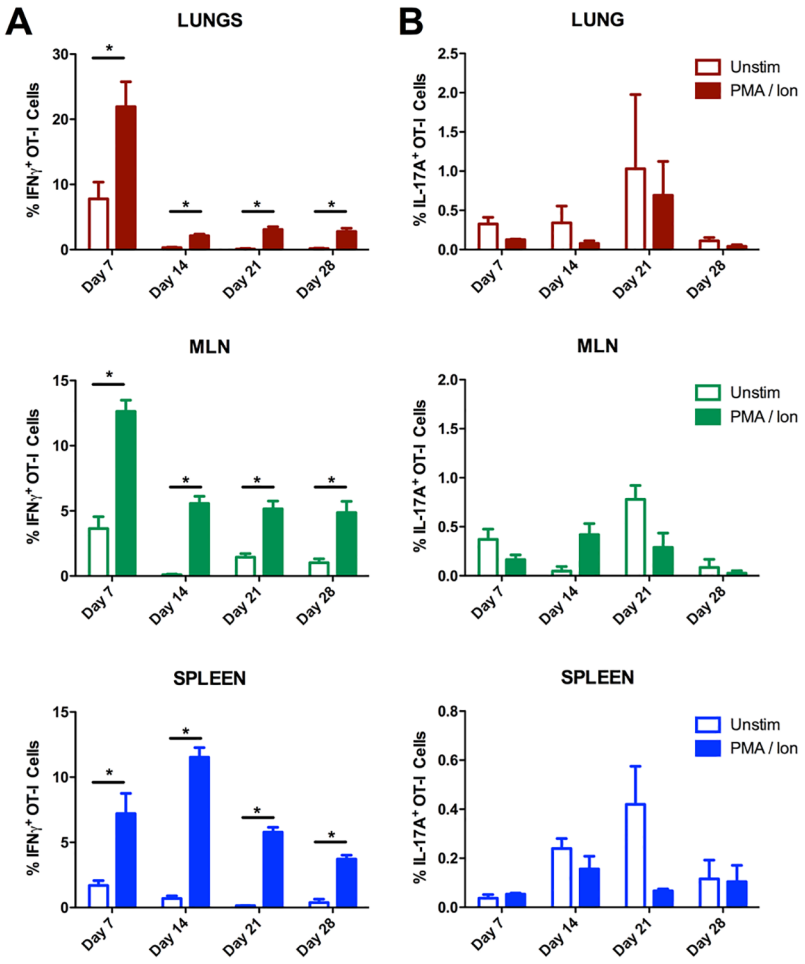

Fig 4. Antigen-specific CD8+ IFN-γ and IL-17A responses during and after LVS-OVA infection. OT-I cells were adoptively transferred into recipient mice 24 hours prior to infection with 1000 CFU of LVS-OVA. Intracellular cytokine staining was performed on single cell suspensions incubated with BrefeldinA, +/- PMA and calcium ionophore. n = 3 per group, means +/- SEM are plotted. * p<0.05 according to two-tailed, unpaired T test.

https://doi.org/10.1371/journal.pone.0190384.g004

Comparison of antigen-specific CD8+ T cell responses to scarification-prime, intranasal-boost versus intranasal-prime, intranasal-boost vaccination strategies

To demonstrate one potential application of LVS-OVA, we studied CD8+ T cell responses in mice primed either intranasally or via scarification, both followed by an intranasal booster. Responses were assessed on day 28 after primary vaccination, and also three and five days after an intranasal booster given on day 30. Mice primed by the intranasal route exhibited significant weight loss before recovering, while mice primed via scarification did not lose weight (Fig 6A). The intranasal booster was well tolerated by both groups (Fig 6B and S1 Fig). On day 28 post-vaccination, similar numbers of OT-I cells were present in the lungs and spleens of both groups (Fig 6C). The MLNs of animals given the intranasal primary vaccination harbored more OT-I cells at this point (Fig 6C). The intranasal booster increased the number of OT-I cells in the MLNs of scarification-primed mice, such that they matched intranasally-primed mice. Additionally, the number of OT-I cells in the lungs of scarification-primed mice

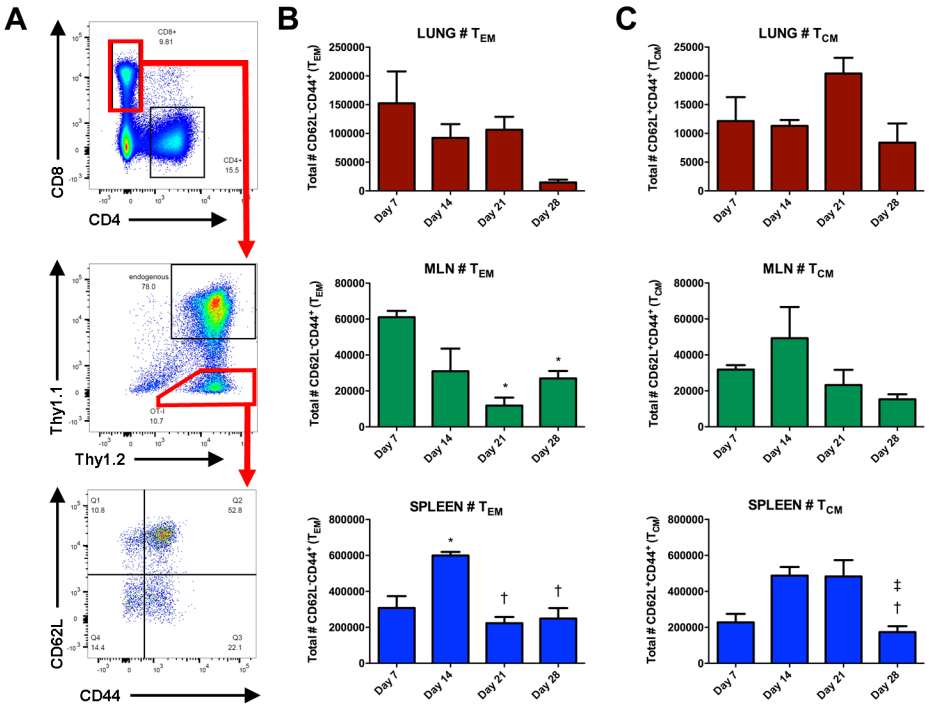

Fig 5. Antigen-specific CD8+ memory T cell development in response to LVS-OVA. OT-I cells were adoptively transferred into recipient mice 24 hours prior to infection with 1000 CFU of LVS-OVA. A) Representative scatterplots demonstrating gating strategy. B) number of T_{EM} OT-I cells. C) number of T_{CM} OT-I cells. n = 3 per group, means +/- SEM are plotted. Statistical significance ($p<0.05$) for one-way ANOVA with Tukey's post test, for the indicated column compared to: * day 7, † day 14, ‡ day 21.

https://doi.org/10.1371/journal.pone.0190384.g005

increased after the booster, reaching significantly higher levels than in intranasally-primed and boosted mice. A similar trend was observed for the numbers of OT-I T_{EM} and T_{CM} cells following priming and booster in both schemes of vaccination (Fig 6D and 6E). Finally, we assessed the number of OT-I cells displaying the resident memory markers CD69 and CD103 within the lungs after these vaccination schemes (Fig 7). For all animals, very few $CD69^+$ $CD103^+$ cells were detected in the lungs, possibly reflecting the poor development of resident memory cells in this model. Altogether, these data suggest that: 1) Intranasal LVS vaccination leads to more antigen-specific $CD8^+$ T cells in the MLN compared to scarification vaccination; 2) an intranasal booster increases the number of antigen-specific $CD8^+$ cells in the MLN and lung of scarification-primed animals, while avoiding the weight loss associated with intranasal primary vaccination; and 3) neither regimen appears to effectively elicit lung-resident $CD8^+$ T cells.

Discussion

There is currently no approved vaccine for the prevention of tularemia, due to concerns regarding the safety and efficacy of existing vaccine candidates. Progress towards a vaccine has been hampered by a lack of understanding of the correlates of protective cell-mediated immunity, in part due to a lack of tools to identify these correlates. Here we report the development of an ovalumbin expression system for *F. tularensis*, which is the first tool to allow for the study of antigen-specific $CD8^+$ T cells in the context of *F. tularensis* infection/vaccination. Our early attempts to express ovalbumin in *F. tularensis* were unsuccessful. However, after codon

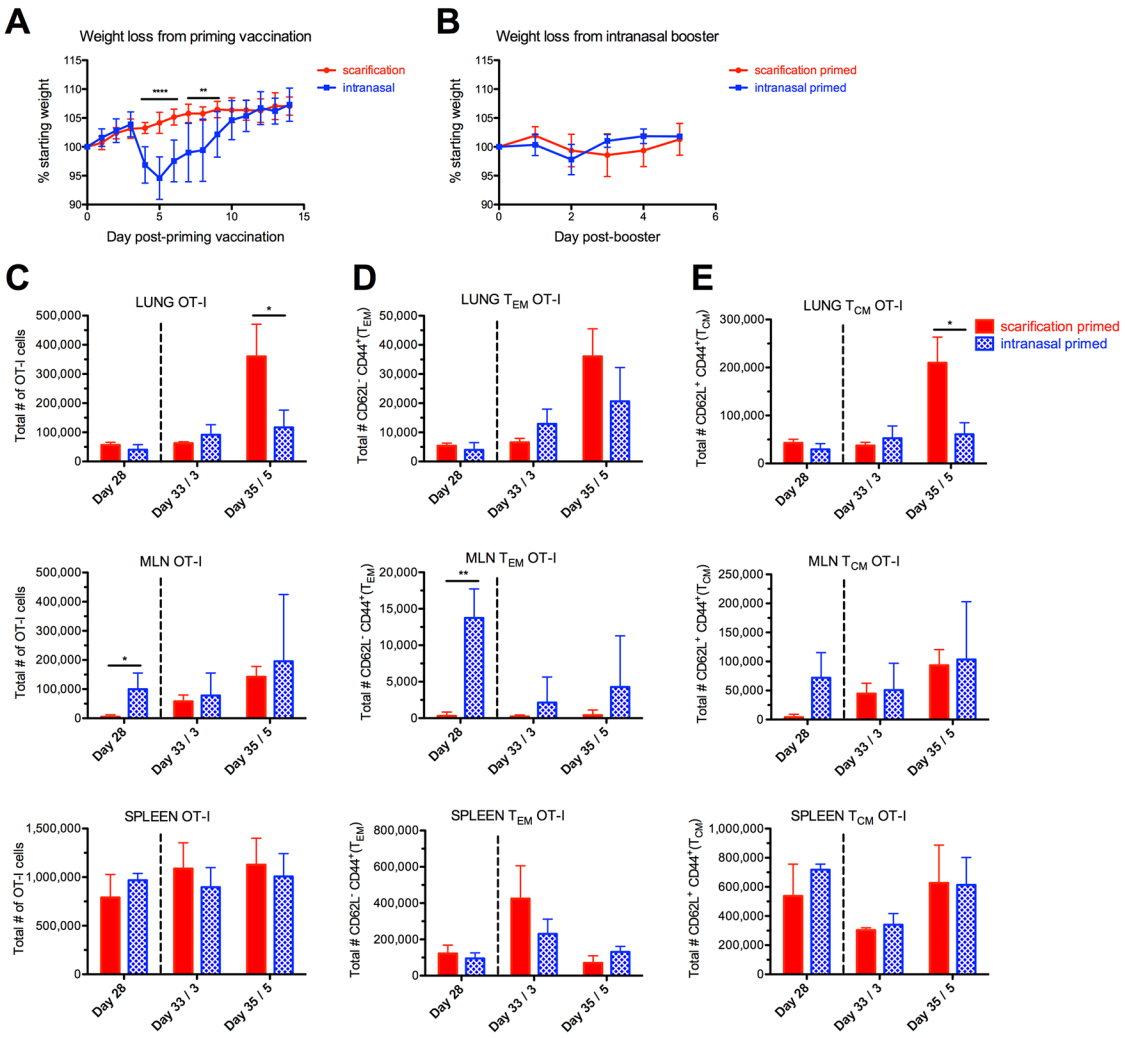

Fig 6. Comparison of antigen-specific CD8+ T cell responses from scarification-prime intranasal-boost, versus intranasal-prime intranasal-boost vaccination strategies. OT-I cells were adoptively transferred into recipient mice, 24 hours prior to priming vaccination with LVS-OVA via the intranasal or scarification route. An intranasal booster was given on day 30. A) weight loss of mice from the priming vaccination. **p<0.01 and ***p<0.001, two-tailed unpaired T test. B) weight of mice following intranasal booster. C-E) The total numbers of OT-I cells (C), T_{EM} OT-I cells (D) and T_{CM} OT-I cells (E) were determined 28 days after priming vaccination, and three and five days after booster (represented by dotted line). Statistical significance was determined by two-tailed, unpaired t-test at each timepoint * p<0.05 ** p<0.01. n = 3 per group, means +/- SD are plotted.

https://doi.org/10.1371/journal.pone.0190384.g006

optimizing a fragment of ovalbumin, and expressing it as a C-terminal tag of the native VgrG protein did we achieve a robust expression (Fig 1A and 1B). A strain of *F. tularensis* LVS containing our expression construct (LVS-OVA) stably maintained the plasmid without selective antibiotics, and stimulated the expansion of adoptively-transferred CD8+ OT-I cells in infected mice.

We first sought to study the initial expansion of CD8+ OT-I cells after intranasal infection. Expansion primarily occurred between days 5–9 (Fig 2); this contrasts with the kinetics observed for another cytosolic bacterial pathogen, *Listeria monocytogenes*, which elicits significant expansion of CD8+ T cells by day 3 [42]. *F. tularensis* employs a stealth strategy that delays activation of innate pro-inflammatory pathways early in the course of infection [10,40,41,43];

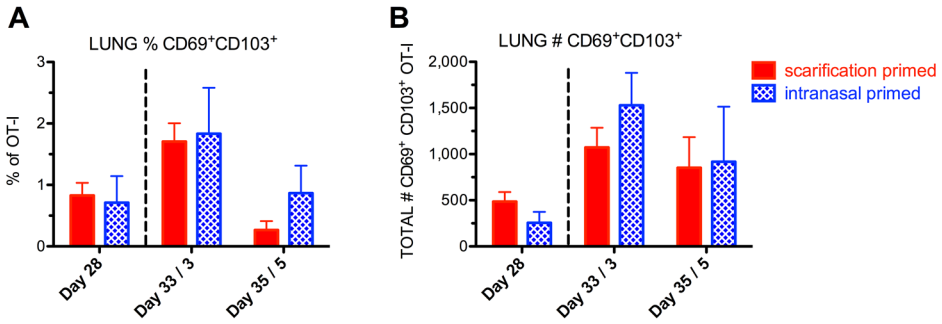

Fig 7. Antigen-specific lung CD8+ T cells with resident memory markers following prime-boost vaccination strategies. A) relative frequency, and B) number of CD69+CD103+ OT-I cells. n = 3 per group, means +/- SD are plotted. No statistically significant differences according to two-tailed, unpaired t-tests.

https://doi.org/10.1371/journal.pone.0190384.g007

these data suggest this stealth strategy may also dramatically affect the kinetics of the T cell response. Our data suggest the peak of the CD8+ T cell response to *F. tularensis* is likely somewhere between day 9 and 14 (Figs 2 and 3). During infection, CD8+ T cells help to eliminate pathogens by killing target cells and producing inflammatory cytokines. We observed that CD8+ OT-I cells produced IFN-γ but not IL-17A upon stimulation, demonstrating LVS-OVA can be used to study antigen-specific CD8+ cytokine responses (Fig 4). In the future, LVS-OVA could be used to determine what other effector molecules are produced by antigen-specific CD8+ T cells, and what vaccination strategies elicit desirable combinations of effector molecules (for instance, polyfunctional cells producing both IFN-γ and TNF-α [20]).

A major advantage of LVS-OVA is that it allows us to study antigen-specific memory development, particularly at times when cells of other specificities may be more abundant. We have observed that CD8+ OT-I T_{CM} and T_{EM} subsets show disparate expansion, contraction and retention properties in various tissues following intranasal LVS infection (Fig 5). Notably, peaks in the T_{EM} population in each organ coincide with peaks in IFN-γ producing cells, and occur around the time bacterial burden is beginning to decline. After clearance of primary infection, T_{EM} are poorly retained in the lungs. The recently described resident memory subset of T cells (T_{RM}) remain in a tissue after the clearance of primary infection, and are thought to provide a rapid response that contributes to protection from reinfection, including against respiratory pathogens [44,45]. However, we detected very few CD8+ OT-I cells expressing the resident memory markers CD69 and CD103 in the lungs of vaccinated mice. This suggests that lung T_{RM} development is poor in this model, and that strategies to boost *F. tularensis*-specific T_{RM} in the lungs may enhance the protectiveness of vaccines. Notably, the generation of lung T_{RM} has been associated with tissue regeneration after injury [45], and the RML strain of LVS, which confers superior protection against virulent strains, has also been shown to be more virulent [10]. It is interesting to speculate that the increased protectiveness of the RML LVS strain may be due to increased generation of *F. tularensis*-specific T_{RM} in the lungs. Studies using our ovalbumin expression system to compare effective and ineffective vaccine responses will help to define correlates protective adaptive immunity.

An ideal vaccine would preferentially induce such protective responses without causing any harm to the host. In this regard, vaccination with *F. tularensis* LVS by the respiratory route appears to provide superior protection compared to other routes [12,19,46,47], but is also associated with significant adverse effects [46]. We used LVS-OVA to compare the CD8+ T cell responses elicited by intranasal vaccination versus skin scarification, a more commonly used route in humans. Mice vaccinated via the intranasal route exhibited significant body weight

loss before recovering, while mice vaccinated via scarification did not lose weight (Fig 6). Intranasal vaccination led to more antigen-specific $CD8^+$ T cells in the lung-draining MLN; however, after an intranasal booster this difference was no longer evident. The intranasal booster also increased the number of antigen-specific $CD8^+$ T cells in the lungs of scarification-primed animals, but they did not lose any weight and tolerated the booster similarly to intranasal-primed animals. One possible implication of these data is that a scarification-prime, respiratory-boost strategy may achieve the same benefits as respiratory vaccination, with enhanced safety.

In summary, we have developed an ovalbumin expression system that allows for the identification and study of antigen-specific $CD8^+$ T cells in the context of *F. tularensis* infection/vaccination. Using an adoptive transfer model, we demonstrate that this tool can be used to study these cells' expansion, effector functions, retention as memory cells, and response to re-challenge or booster vaccinations. The availability of this system opens up a number of possibilities for critical detailed studies, including how $CD8^+$ T cell responses vary based on *F. tularensis* strain, route of inoculation, available cytokines, and how adjuvants may enhance these responses. Ultimately, such studies will enhance our understanding of protective adaptive immunity, and helping to lay the foundation for the development of a safe and effective vaccine for the prevention of tularemia.

Supporting information

S1 Fig. Bacterial burdens following intranasal booster. Mice (n = 3 per group) were given a priming vaccination of LVS-OVA via the scarification or intranasal route, followed by a booster with 10,000 CFU on day 30. Bacterial burdens are shown on day 3 and day 5 after the booster.
(TIF)

Acknowledgments

We sincerely thank Dr. Karl Klose, University of Texas San Antonio for providing plasmid pKK214. We also thank The Huck Institutes of the Life Sciences for the facilities and technical support.

Author Contributions

Conceptualization: David E. Place, David R. Williamson, Surojit Sarkar, Vandana Kalia, Girish S. Kirimanjeswara.

Formal analysis: David E. Place, David R. Williamson, Yevgeniy Yuzefpolskiy, Surojit Sarkar, Girish S. Kirimanjeswara.

Funding acquisition: Girish S. Kirimanjeswara.

Investigation: David E. Place, David R. Williamson, Yevgeniy Yuzefpolskiy, Bhuvana Katkere, Girish S. Kirimanjeswara.

Methodology: David E. Place, David R. Williamson, Bhuvana Katkere, Surojit Sarkar, Vandana Kalia, Girish S. Kirimanjeswara.

Project administration: Girish S. Kirimanjeswara.

Resources: Girish S. Kirimanjeswara.

Supervision: Girish S. Kirimanjeswara.

Validation: Girish S. Kirimanjeswara.

Writing – original draft: David E. Place, David R. Williamson, Girish S. Kirimanjeswara.

References

1. Saslaw S, Eigelsbach H, Prior J, Wilson H, Carhart S. Tularemia vaccine study: II. respiratory challenge. Arch Intern Med. 1961; 107: 702–714. https://doi.org/10.1001/archinte.1961.03620050068007 PMID: 13746667
2. Sjöstedt A. Tularemia: history, epidemiology, pathogen physiology, and clinical manifestations. Ann N Y Acad Sci. 2007; 1105: 1–29. https://doi.org/10.1196/annals.1409.009 PMID: 17395726
3. Faith SA, Smith LP, Swatland AS, Reed DS. Growth conditions and environmental factors impact aerosolization but not virulence of Francisella tularensis infection in mice. Front Cell Infect Microbiol. 2012; 2: 1–10.
4. Harris S. Japanese Biological Warfare Research on Humans: A Case Study of Microbiology and Ethics. Ann N Y Acad Sci. 1992; 666: 21–52. PMID: 1297279
5. Christopher LGW, Cieslak LTJ, Pavlin JA, Eitzen EM. Biological Warfare: A Historical Perspective. JAMA. 1997; 278: 412–417. https://doi.org/10.1001/jama.1997.03550050074036 PMID: 9244333
6. Oyston PCF, Sjöstedt A, Titball RW. Tularaemia: bioterrorism defence renews interest in Francisella tularensis. Nat Rev Microbiol. 2004; 2: 967–978. https://doi.org/10.1038/nrmicro1045 PMID: 15550942
7. Eigelsbach HT, Downs CM. Prophylactic Effectiveness of Live and Killed Tularemia Vaccines. J Immunol. 1961; 87: 415–425. PMID: 13889609
8. Eigelsbach HT, Braun W, Herring RD. Studies on the variation of Bacterium tularense. J Bacteriol. 1951; 61: 557–569. PMID: 14832199
9. Hartley G, Taylor R, Prior J, Newstead S, Hitchen PG, Morris HR, et al. Grey variants of the live vaccine strain of Francisella tularensis lack lipopolysaccharide O-antigen, show reduced ability to survive in macrophages and do not induce protective immunity in mice. Vaccine. 2006; 24: 989–996. https://doi.org/10.1016/j.vaccine.2005.08.075 PMID: 16257097
10. Griffin AJ, Crane DD, Wehrly TD, Bosio CM. Successful Protection against Tularemia in C57BL/6 Mice Is Correlated with Expansion of Francisella tularensis-Specific Effector T Cells. Clin Vaccine Immunol CVI. 2015; 22: 119–128. https://doi.org/10.1128/CVI.00648-14 PMID: 25410207
11. Cherwonogrodzky JW, Knodel MH, Spence MR. Increased encapsulation and virulence of Francisella tularensis live vaccine strain (LVS) by subculturing on synthetic medium. Vaccine. 1994; 12: 773–775. https://doi.org/10.1016/0264-410X(94)90284-4 PMID: 7975855
12. Wayne Conlan J, Shen H, KuoLee R, Zhao X, Chen W. Aerosol-, but not intradermal-immunization with the live vaccine strain of Francisella tularensis protects mice against subsequent aerosol challenge with a highly virulent type A strain of the pathogen by an αβ T cell- and interferon gamma- dependent mechanism. Vaccine. 2005; 23: 2477–2485. https://doi.org/10.1016/j.vaccine.2004.10.034 PMID: 15752834
13. Roberts LM, Wehrly TD, Crane DD, Bosio CM. Expansion and retention of pulmonary CD4+ T cells after prime boost vaccination correlates with improved longevity and strength of immunity against tularemia. Vaccine. 2017; 35: 2575–2581. https://doi.org/10.1016/j.vaccine.2017.03.064 PMID: 28372827
14. Ray HJ, Cong Y, Murthy AK, Selby DM, Klose KE, Barker JR, et al. Oral Live Vaccine Strain-Induced Protective Immunity against Pulmonary Francisella tularensis Challenge Is Mediated by CD4+ T Cells and Antibodies, Including Immunoglobulin A. Clin Vaccine Immunol. 2009; 16: 444–452. https://doi.org/10.1128/CVI.00405-08 PMID: 19211773
15. Saslaw S, Carhart S. Studies with tularemia vaccines in volunteers. III. Serologic aspects following intracutaneous or respiratory challenge in both vaccinated and nonvaccinated volunteers. Am J Med Sci. 1961; 241: 689–699. PMID: 13746662
16. Tärnvik A. Nature of Protective Immunity to Francisella tularensis. Rev Infect Dis. 1989; 11: 440–451. https://doi.org/10.1093/clinids/11.3.440 PMID: 2665002
17. Allen WP. Immunity against tularemia: passive protection of mice by transfer of immune tissues. J Exp Med. 1962; 115: 411–420. PMID: 13860583
18. Fulop M, Mastroeni P, Green M, Titball RW. Role of antibody to lipopolysaccharide in protection against low- and high-virulence strains of Francisella tularensis. Vaccine. 2001; 19: 4465–4472. https://doi.org/10.1016/S0264-410X(01)00189-X PMID: 11483272
19. Wu TH, Hutt JA, Garrison KA, Berliba LS, Zhou Y, Lyons CR. Intranasal Vaccination Induces Protective Immunity against Intranasal Infection with Virulent Francisella tularensis Biovar A. Infect Immun. 2005; 73: 2644–2654. https://doi.org/10.1128/IAI.73.5.2644-2654.2005 PMID: 15845466

20. Roberts LM, Crane DD, Wehrly TD, Fletcher JR, Jones BD, Bosio CM. Inclusion of Epitopes That Expand High-Avidity CD4+ T Cells Transforms Subprotective Vaccines to Efficacious Immunogens against Virulent Francisella tularensis. J Immunol. 2016; 197: 2738–2747. https://doi.org/10.4049/jimmunol.1600879 PMID: 27543611

21. Khan SH, Badovinac VP. Listeria monocytogenes: a model pathogen to study antigen-specific memory CD8 T cell responses. Semin Immunopathol. 2015; 37: 301–310. https://doi.org/10.1007/s00281-015-0477-5 PMID: 25860798

22. Sims S, Willberg C, Klenerman P. MHC-peptide tetramers for the analysis of antigen-specific T cells. Expert Rev Vaccines. 2010; 9: 765–774. https://doi.org/10.1586/erv.10.66 PMID: 20624049

23. Clarke SRm, Barnden M, Kurts C, Carbone FR, Miller JF, Heath WR. Characterization of the ovalbumin-specific TCR transgenic line OT-I: MHC elements for positive and negative selection. Immunol Cell Biol. 2000; 78: 110–117. https://doi.org/10.1046/j.1440-1711.2000.00889.x PMID: 10762410

24. LoVullo ED, Molins-Schneekloth CR, Schweizer HP, Pavelka MS. Single-copy chromosomal integration systems for Francisella tularensis. Microbiology. 2009; 155: 1152–1163. https://doi.org/10.1099/mic.0.022491-0 PMID: 19332817

25. Puigbò P, Guzmán E, Romeu A, Garcia-Vallvé S. OPTIMIZER: a web server for optimizing the codon usage of DNA sequences. Nucleic Acids Res. 2007; 35: W126–W131. https://doi.org/10.1093/nar/gkm219 PMID: 17439967

26. Kuoppa K, Forsberg Å, Norqvist A. Construction of a reporter plasmid for screening in vivo promoter activity in Francisella tularensis. FEMS Microbiol Lett. 2001; 205: 77–81. https://doi.org/10.1111/j.1574-6968.2001.tb10928.x PMID: 11728719

27. Abd H, Johansson T, Golovliov I, Sandström G, Forsman M. Survival and Growth of Francisella tularensis in Acanthamoeba castellanii. Appl Environ Microbiol. 2003; 69: 600–606. https://doi.org/10.1128/AEM.69.1.600-606.2003 PMID: 12514047

28. Zaide G, Grosfeld H, Ehrlich S, Zvi A, Cohen O, Shafferman A. Identification and Characterization of Novel and Potent Transcription Promoters of Francisella tularensis. Appl Environ Microbiol. 2011; 77: 1608–1618. https://doi.org/10.1128/AEM.01862-10 PMID: 21193666

29. Maier TM, Havig A, Casey M, Nano FE, Frank DW, Zahrt TC. Construction and Characterization of a Highly Efficient Francisella Shuttle Plasmid. Appl Environ Microbiol. 2004; 70: 7511–7519. https://doi.org/10.1128/AEM.70.12.7511-7519.2004 PMID: 15574954

30. Quah BJC, Parish CR. The Use of Carboxyfluorescein Diacetate Succinimidyl Ester (CFSE) to Monitor Lymphocyte Proliferation. J Vis Exp. 2010; https://doi.org/10.3791/2259 PMID: 20972413

31. Quah BJC, Parish CR. New and improved methods for measuring lymphocyte proliferation in vitro and in vivo using CFSE-like fluorescent dyes. J Immunol Methods. 2012; 379: 1–14. https://doi.org/10.1016/j.jim.2012.02.012 PMID: 22370428

32. Hamada H, Garcia-Hernandez M de la L, Reome JB, Misra SK, Strutt TM, McKinstry KK, et al. Tc17, a Unique Subset of CD8 T Cells That Can Protect against Lethal Influenza Challenge. J Immunol. 2009; 182: 3469–3481. https://doi.org/10.4049/jimmunol.0801814 PMID: 19265125

33. Mittrücker H-W, Visekruna A, Huber M. Heterogeneity in the Differentiation and Function of CD8+ T Cells. Arch Immunol Ther Exp (Warsz). 2014; 62: 449–458. https://doi.org/10.1007/s00005-014-0293-y PMID: 24879097

34. Edwards JA, Rockx-Brouwer D, Nair V, Celli J. Restricted cytosolic growth of Francisella tularensis subsp. tularensis by IFN-γ activation of macrophages. Microbiology. 2010; 156: 327–339. https://doi.org/10.1099/mic.0.031716-0 PMID: 19926654

35. Holická M, Novosad J, Loudová M, Kudlová M, Krejsek J. The effect of interferon-gamma and lipopolysaccharide on the growth of Francisella tularensis LVS in murine macrophage-like cell line J774. Acta Medica (Hradec Kralove). 2009; 52: 101–106.

36. Roberts LM, Davies JS, Sempowski GD, Frelinger JA. IFN-γ, but not IL-17A, is required for survival during secondary pulmonary Francisella tularensis Live Vaccine Stain infection. Vaccine. 2014; 32: 3595–3603. https://doi.org/10.1016/j.vaccine.2014.05.013 PMID: 24837506

37. Nolz JC. Molecular mechanisms of CD8+ T cell trafficking and localization. Cell Mol Life Sci. 2015; 72: 2461–2473. https://doi.org/10.1007/s00018-015-1835-0 PMID: 25577280

38. Roberts AD, Ely KH, Woodland DL. Differential contributions of central and effector memory T cells to recall responses. J Exp Med. 2005; 202: 123–133. https://doi.org/10.1084/jem.20050137 PMID: 15983064

39. Sallusto F, Geginat J, Lanzavecchia A. Central memory and effector memory T cell subsets: function, generation, and maintenance. Annu Rev Immunol. 2004; 22: 745–763. https://doi.org/10.1146/annurev.immunol.22.012703.104702 PMID: 15032595

40. Bosio CM, Bielefeldt-Ohmann H, Belisle JT. Active Suppression of the Pulmonary Immune Response by Francisella tularensis Schu4. J Immunol. 2007; 178: 4538–4547. https://doi.org/10.4049/jimmunol.178.7.4538 PMID: 17372012

41. Conlan JW, Zhao X, Harris G, Shen H, Bolanowski M, Rietz C, et al. Molecular immunology of experimental primary tularemia in mice infected by respiratory or intradermal routes with type A Francisella tularensis. Mol Immunol. 2008; 45: 2962–2969. https://doi.org/10.1016/j.molimm.2008.01.022 PMID: 18321578

42. Foulds KE, Zenewicz LA, Shedlock DJ, Jiang J, Troy AE, Shen H. Cutting Edge: CD4 and CD8 T Cells Are Intrinsically Different in Their Proliferative Responses. J Immunol. 2002; 168: 1528–1532. https://doi.org/10.4049/jimmunol.168.4.1528 PMID: 11823476

43. Andersson H, Hartmanová B, Kuolee R, Rydén P, Conlan W, Chen W, et al. Transcriptional profiling of host responses in mouse lungs following aerosol infection with type A Francisella tularensis. J Med Microbiol. 2006; 55: 263–271. https://doi.org/10.1099/jmm.0.46313-0 PMID: 16476789

44. McMaster SR, Wilson JJ, Wang H, Kohlmeier JE. Airway-Resident Memory CD8 T Cells Provide Antigen-Specific Protection against Respiratory Virus Challenge through Rapid IFN-γ Production. J Immunol. 2015; 195: 203–209. https://doi.org/10.4049/jimmunol.1402975 PMID: 26026054

45. Takamura S, Yagi H, Hakata Y, Motozono C, McMaster SR, Masumoto T, et al. Specific niches for lung-resident memory CD8+ T cells at the site of tissue regeneration enable CD69-independent maintenance. J Exp Med. 2016; 213: 3057–3073. https://doi.org/10.1084/jem.20160938 PMID: 27815325

46. Hornick RB, Eigelsbach HT. Aerogenic immunization of man with live Tularemia vaccine. Bacteriol Rev. 1966; 30: 532–538. PMID: 5917334

47. Eigelsbach HT, Tulis JJ, Overholt EL, Griffith WR. Aerogenic immunization of the monkey and guinea pig with live tularemia vaccine. Exp Biol Med. 1961; 108: 732–734.